

Supplementary Information

Charge transfer from internal electrostatic fields is superior to surface defects for the 2, 4- dichlorophenol degradation in $K_{3-x}Na_xB_6O_{10}Br$ photocatalysts

Xiaoyun Fan*^a, Yang Zhang ^a, Kangdi Zhong ^b

^a School of Environment, Jinan University, Guangzhou 510632, China

^b Department of Physics, Changji University, Changji, 830011, China.

E-mail: xyfan@jun.edu.cn;

1.1 Photoelectron chemical (PEC) measurements The photocurrents of UV-Vis light on and off studies were determined on a CHI660E electrochemical system using a standard three-electrode cell with a working electrode (10 mm ×10 mm), a platinum plate as the counter electrode, and a standard calomel electrode (SCE) as the reference electrode. The KBB film was prepared on ITO glass, followed by air-drying. The experiments were performed in a 50 mL quartz cylinder reactor which was placed in front of a xenon lamp ($\lambda > 320$ nm; Perfect Light Company, Beijing, China). The photoelectron chemical (PEC) activities of the samples were all evaluated in a 0.1 M Na₂SO₄ solution.

1.2 Photocatalytic Activity. Typically, 50 mg catalysts were added into 100 mL aqueous solution of 2, 4-DCP (50 mg / L) in a 250 mL glass beaker, then stirred for 20 min in the dark to attain adsorption equilibrium, and irradiated by a xenon lamp (the light intensity at the test samples= 0.185 W/cm²). The percentage of residual contaminants solution at a selected time of irradiation is given by C/C_0 , where C_0 is the concentration of the contaminants solution at the initial stage, and C is the concentration at selected irradiation times. To test the reproducibility and uncertainty of the degradation experiments, the photochemical reactions were repeated four times.

1.3 Structure description. For an ideal ABO₃-type perovskite structure, such as CaTiO₃, the corners of the cubic cell are occupied by Ca²⁺ ions with coordination number 12, and the sites of the face centers are occupied by O²⁻ ions with coordination number 6, while the bulk center is occupied by a Ti⁴⁺ ion with coordination number 6. Ti⁴⁺ and six neighboring O²⁻ ions form an octahedron TiO₆, as schematically drawn in Figure S1a. The structure exhibits an intricate three-dimensional network composed of [B₆O₁₀] units and [BrK₆] octahedra (Figure S1b) and can also be described as two networks (a [B₆O₁₀]_∞ and a BrK₆ net) that are interweaved. By analogy with the mineral perovskite CaTiO₃, the positions of large calcium cations are occupied by the [B₆O₁₀] groups, the positions of titanium atoms are similar to those of bromine atoms, and the positions of oxygen atoms are similar to the positions of potassium atoms. Here, for the perovskite compounds KBB1, the site of the bulk center is occupied by [B₆O₁₀] in a charge-balanced manner, which has been widely investigated in ferroelectric materials.

With the variation of the ionic radius of Br^- and K^+ , the crystal structure of ABO_3 perovskite will be subjected to some distortion, Hence, their formulas can be represented as $[\text{B}_6\text{O}_{10}]\text{BrK}_3$.

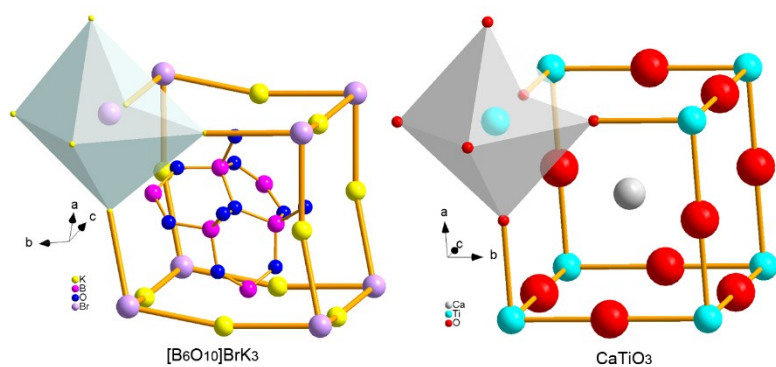


Figure S1. Similarity of the KBB1-KBB3 crystal structure and the classic R3m perovskite structure of CaTiO₃ compound.

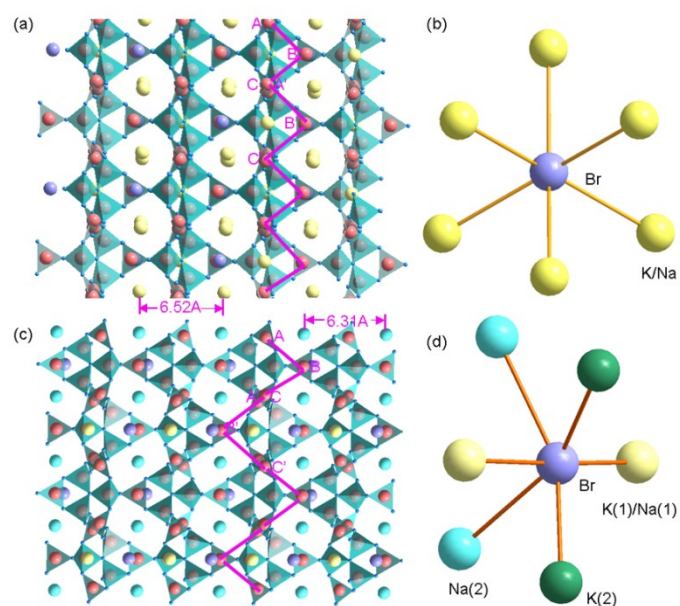


Figure S2. 3D framework of the KBB3 crystal (a) and KBB4 crystal(c), The coordination environment of Br in the KBB3 sample(b) and KBB4 sample(d).

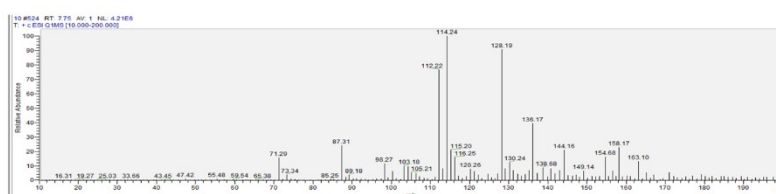
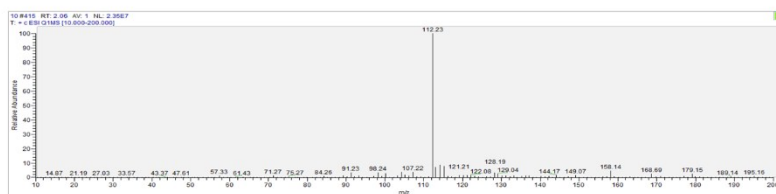
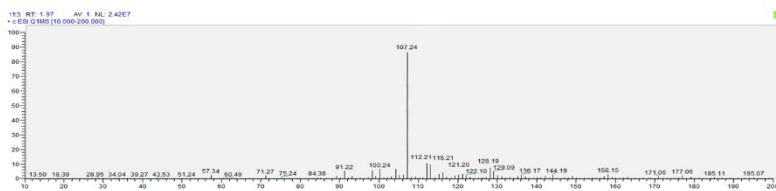
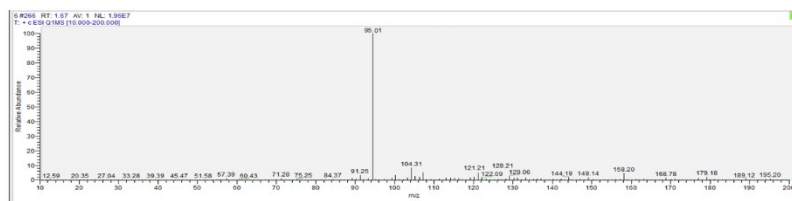
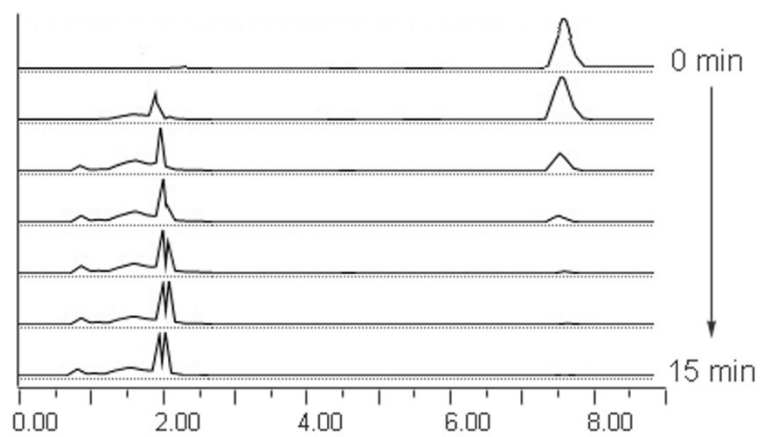


Figure S3. HPLC and LC-MS of 2, 4-DCP ($R_t \approx 7.3$ -7.8 min) by using KBB3 sample under UV-vis light irradiation.

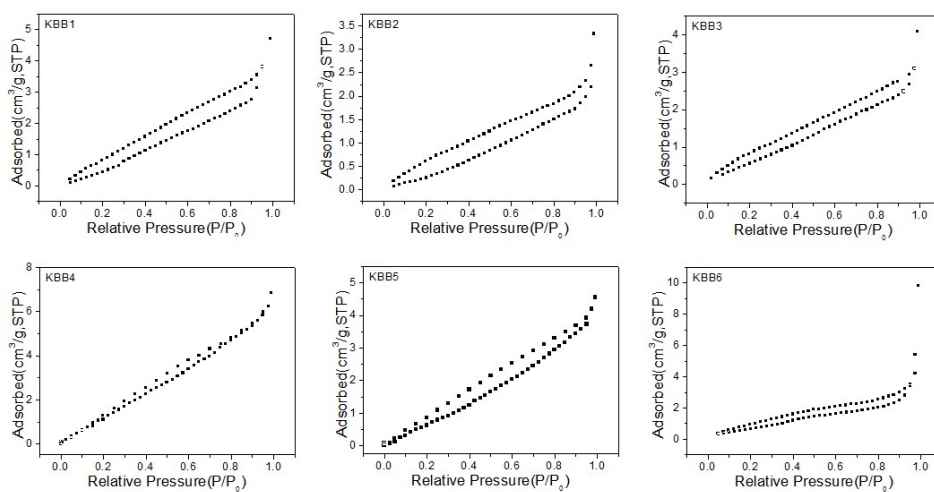


Figure S4. Nitrogen adsorption-desorption isotherms of KBB1-KBB6 samples.

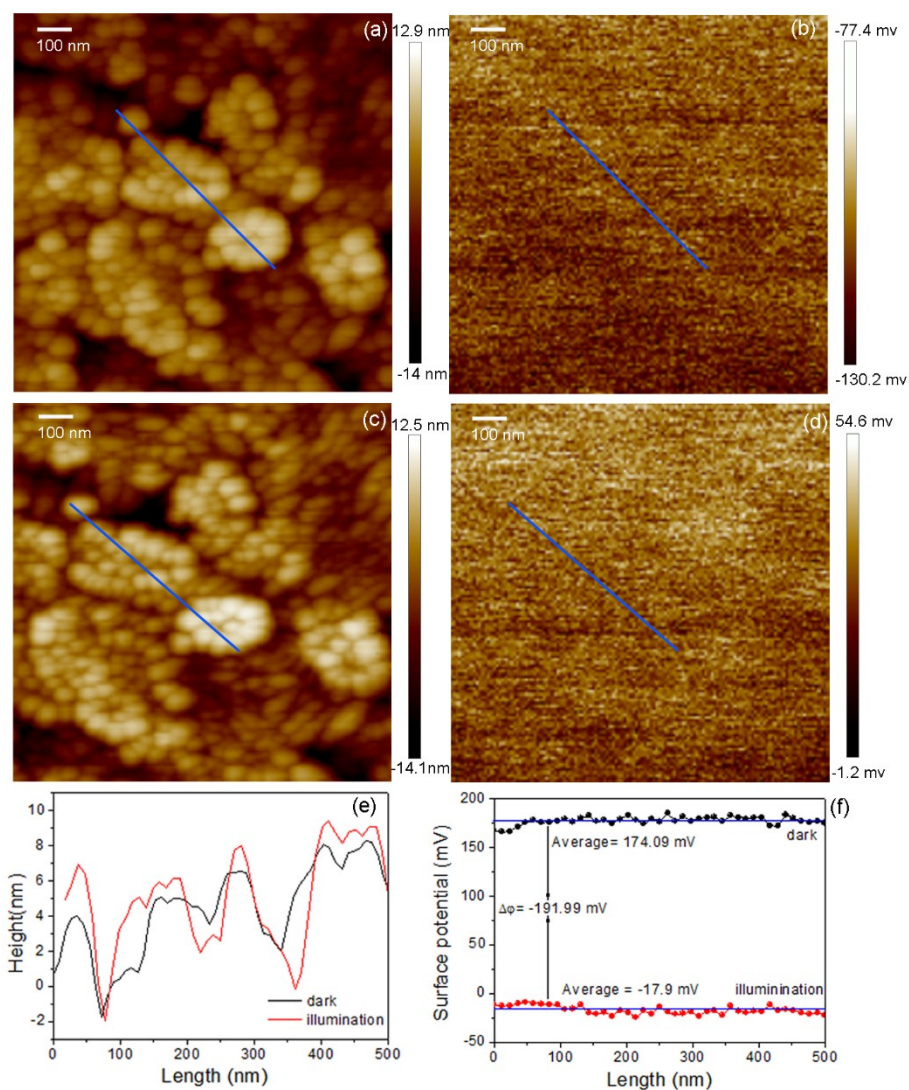


Figure S5. AFM images of KBB3 before (a) and after (c) UV-visible light irradiation and corresponding surface potential images of KBB3 before (b) and after (d) UV-visible light irradiation. (e) Height differential curve along the blue line from panel a and panel c. (f) Surface potential profile along the blue line in panel b and panel d.

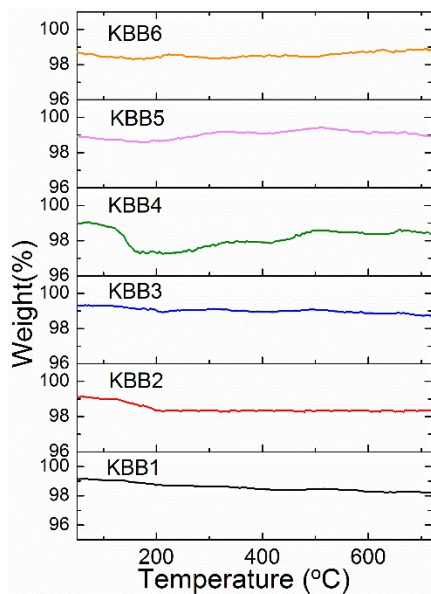


Figure S6. The TGA curve for the KBB1-KBB6 samples in the air.

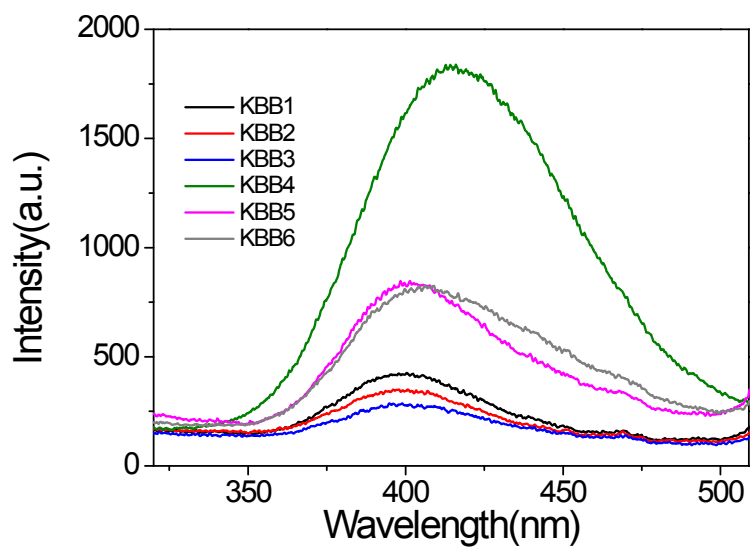


Figure S7. Photo luminescence spectra of the KBB1-KBB6 samples.

Table S1. Raman shifts, IR frequency (cm^{-1}) and the assignment of vibrational modes of the KBB1-KBB6 photocatalyst.

Raman frequency		IR frequency		Vibrational modes
KBB1- KBB3	KBB4- KBB6	KBB1- KBB3	KBB4- KBB6	
58-105	176- 72	-	-	Lattice vibration
238-347	240-363	564,567	521,575	BO_4 bond bending
597-478	445-590	594	593	BO_4 symmetric vibration
630-750	630-716	681-731	624-788	BO_3 bending vibration
809	800-823	826-990	853-896	BO_3 symmetric stretch
1001-1149	1015-1169	1162-1167	1077-1185	BO_4 asymmetric stretch
1312	1349	1299	1317	BO_3 asymmetric stretch

Table S2. LC-MS data of photodegraded products of 2, 4-DCP by using KBB3 sample.

Retention time (min)	Mw (m/z)	Assignment	CAS no.
7.55	163.10	2, 4- dichlorophenol	120-83-2
2.06	112.23	Catechol	120-80-9
1.97	107.24	1,4-Benzoquinone	106-51-4
1.67	95.01	Phenol	108-95-2